NeuroImage 119 (2015) 13–19

Contents lists available at ScienceDirect

NeuroImage

journal homepage: www.elsevier.com/locate/ynimg

Beta oscillations and reward processing: Coupling oscillatory activity and hemodynamic responses

Ernest Mas-Herrero [a,1], Pablo Ripollés [a,b,1], Azadeh HajiHosseini [c], Antoni Rodríguez-Fornells [a,b,d], Josep Marco-Pallarés [a,b,*]

[a] Cognition and Brain Plasticity Group [Bellvitge Biomedical Research Institute] IDIBELL, L'Hospitalet de Llobregat, Barcelona 08097, Spain
[b] Dept. of Basic Psychology, University of Barcelona, Barcelona 08097, Spain
[c] Dept. of Psychology, University of Victoria, P. O. Box 1700 STN CSC, Victoria, BC V8W 2Y2, Canada
[d] Catalan Institution for Research and Advanced Studies, ICREA, Barcelona 08010, Spain

ARTICLE INFO

Article history:
Received 16 December 2014
Accepted 21 May 2015
Available online 10 June 2015

Keywords:
Reward
Beta oscillations
fMRI
Time–frequency
JointICA

ABSTRACT

Diverse cortical and subcortical regions are synergically engaged during reward processing. Previous studies using time–frequency decomposition of Electroencephalography (EEG) data have revealed an increase of mid-frontal beta oscillatory activity (BOA) after reward delivery, which could be a potential mechanism in the coordination of the different areas engaged during reward processing. In order to evaluate this hypothesis, twenty subjects performed a monetary gambling paradigm in two separate sessions (EEG and fMRI). Time–frequency oscillatory EEG data and fMRI activity were fused using Joint Independent Component Analysis (ICA). The present results showed that mid-frontal BOA elicited by monetary gains is associated with the engagement of a fronto–striatal–hippocampal network previously involved in reward-related memory enhancement, supporting the role of this activity during reward processing.

Introduction

Learning on the bases of reward is critical to anticipate potential outcomes and optimize decision-making. This fundamental process requires the dynamic interplay of distributed neural substrates involved in reward, attention and memory (Dayan and Balleine, 2002). In this vein, previous studies have shown that fronto–striatal–hippocampal interactions play an important role in the enhancement of both long and short-term memory formation induced by rewards (Wittmann et al., 2005, 2008; Adcock et al., 2006; Murty and Adcock, 2013). The optimal engagement of such extensive network requires of an integrative mechanism that allows the selective recruitment and rapid coordination of the brain structures involved in it. One potential mechanism to achieve such efficient neuronal communication is the synchronization of separated brain areas to a common rhythm of neuronal firing (von Stein and Sarnthein, 2000). Concretely, Beta Oscillatory Activity (BOA) has recently been suggested to be a key component mediating the cross-talk between reward, memory and attention processes following rewarding events (Marco-Pallarés et al., 2014).

Previous Electroencephalography (EEG) and Magnetoencephalography (MEG) human studies using time–frequency (TF) decomposition have revealed a mid-frontal BOA elicited by positive outcomes (20–30 Hz, peaking 200–400 ms after positive feedback; Cohen et al., 2007; Marco-Pallarés et al., 2008; Marco-Pallarés et al., 2009; Cunillera et al., 2012; HajiHosseini et al., 2012; Leicht et al., 2013; Luft et al., 2013; Padrao et al., 2013) and reward-predicting cues (Bunzeck et al., 2011; Kawasaki and Yamaguchi, 2013; Apitz and Bunzeck, 2014). This gain-related signal has been associated to the engagement of reward-related brain networks due to the fact that BOA shows a similar pattern in response to rewards than that observed in midbrain dopaminergic and striatal neurons. Interestingly, several studies have supported this view. Indeed, BOA has been shown to be sensitive to individual differences in the Catechol-O-methyltransferase enzyme (COMT) polymorphism (Marco-Pallarés et al., 2009), which is related to differences in dopamine levels. Similarly, administration of dopaminergic agonists also modulates BOA in response to reward-predicting cues and reward outcomes (Apitz and Bunzeck, 2014). In line with these results, Leicht and colleagues (2013) showed that individual differences in BOA predicted participants' sensation seeking trait, strongly related to increased dopaminergic activity (Blanchard et al., 2009). All in all, these studies point out the relevance of the mesolimbic system in the modulation of cortical BOA.

Although most of these studies have focused on local power results, several authors have hypothesized that this activity may be related to long-rage communication driven by phase synchronization (Cohen et al., 2011; Marco-Pallarés et al., 2014). In particular, Marco-Pallarés and colleagues (2014) have proposed that BOA may reflect the

* Corresponding author at: Department of Basic Psychology—IDIBELL, L'Hospitalet de Llobregat, University of Barcelona, Campus Bellvitge, Barcelona 08097, Spain.
E-mail address: josepmarco@gmail.com (J. Marco-Pallarés).
[1] Both authors equally contributed to this work.

http://dx.doi.org/10.1016/j.neuroimage.2015.05.095
1053-8119/

transmission of fast motivational value signals from cortical structures to downstream regions in order to enhance the encoding of positive or novel events. Accordingly, BOA has also been related to working memory improvements in rewarding motivational contexts (Kawasaki and Yamaguchi, 2013), a process mediated by fronto–striatal–hippocampal loops (Murty and Adcock, 2013). Thus, according to Marco-Pallarés and colleagues' model, BOA would reflect the interplay between attentional (orienting attention to relevant on-going goals), motivational (enhancing encoding) and memory circuits (storing information). However, this assumption has never been tested.

Uncovering cerebral networks underlying BOA would involve the use of a combination of neuroimaging techniques with both high temporal precision—needed to derive BOA ranges—and also optimal spatial resolution, along with the ability to assess distant brain regions with no a priori constrains. A possible approach to tackle the aforementioned technical difficulties is the use of a combined EEG-fMRI analysis which would take advantage of the optimal temporal and spatial precision provided by each neuroimaging technique, respectively (Carlson et al., 2011). Independent Component Analysis (ICA)—a multivariate, data-driven approach— has emerged as a promising method to extract and combine temporal information from EEG and spatial information from fMRI. In particular, Joint ICA (Calhoun et al., 2006) selects independent components from different neuroimaging techniques simultaneously, using, for example, EEG data in the temporal domain and fMRI activation maps in the spatial domain (Calhoun et al., 2009). In the present study—by performing a multimodal Joint ICA EEG-fMRI analysis—we aimed to test the hypothesis that mid-frontal BOA is associated with reward-related networks.

Materials and Methods

Participants

Twenty students (M = 22.9 years old, SD = 2.9, 15 women) participated in the experiment. All participants were paid 10€ per hour plus an amount of monetary bonus depending on participants' performance. All participants gave written informed consent and all procedures were approved by the local ethical committee.

Experimental Procedure

Each participant performed a separated fMRI and EEG session (as in the EEG-fMRI gambling setup of Carlson et al., 2011). Participants performed the same gambling task in both sessions adapted to EEG and fMRI setups. The EEG session was performed in a different room to that of the scanner. The order of the two sessions was counterbalanced across participants and was separated by at least 1 day (M = 8.2, SD = 7.5 days).

Participants were engaged in a gambling task (see Fig. 1), similar to the one used in the study by HajiHosseini et al. (2012). Each trial started with a figure (pre-cue) which indicated whether the next cue would be informative (information pre-cue followed by informative cue) or not (non-information pre-cue followed by non-informative cue). If the trial was informative, one of two possible cues appeared ($p = 0.5$); a cue indicating either high probability (hp) or low probability (lp) of monetary wins. However, if the pre-cue indicated that the trial was non-informative, one of two different cues with no relationship with the probability of winning or losing or the final result of the trial (gain or loss) was randomly presented ($p = 0.5$). In other words, cues in the non-informative trials provided no information and were displayed to maintain a consistent structure across the two conditions (information vs. non-information). In the fMRI task, the pre-cue and cue lasted 8 s with a pseudorandom jitter from a fixed distribution between −1 and 1 s at 125 ms steps. This jitter was added both to the pre-cue and subtracted from the cue (i.e., the pre-cue lasted 4 s plus the jitter and the cue 4 s minus the jitter, for a total of 8 s). In the EEG task, the time between the pre-cue and the cue signals and the time between the cue signal and the presentation of the cards was set to 1.5 s (for a total of 3 s).

After the presentation of the cue (high probability, low probability, or the non-informative random cue), four blank cards appeared on the screen. Subjects were instructed to select a card among four by pressing one of four buttons (two buttons in each hand). After the response choice, the selected card was marked and after 2 s all cards turned to either green or red. If the subject had selected a green card, he/she won 50 euro cents whereas if the participant had selected a red card, he/she lost 50 euro cents. If a participant did not respond after 2 s, a message prompting him/her to respond faster was presented and no money was lost/won (no red/green cards were shown). In high probability trials, three cards turned green and one turned red, whereas in low probability trials three cards turned red and one turned green. In non-informative conditions, the same pattern of results occurred: in half of the trials three cards turned red and one green and in the other half three turned green and one red. After the presentation of feedback, a blank screen was presented for 2 s, indicating the beginning of a new trial. The feedback indicating the win or the loss remained in the screen for 2 s in the fMRI task and 1.5 s in the EEG task. In addition, in the fMRI task, a jitter between −1 and 1 s at 125 ms steps, was added to the selection of the card and subtracted from the blank screen separating the different trials (i.e., the selection of the card lasted 2 s plus the jitter and the time between trials lasted 2 s minus the jitter).

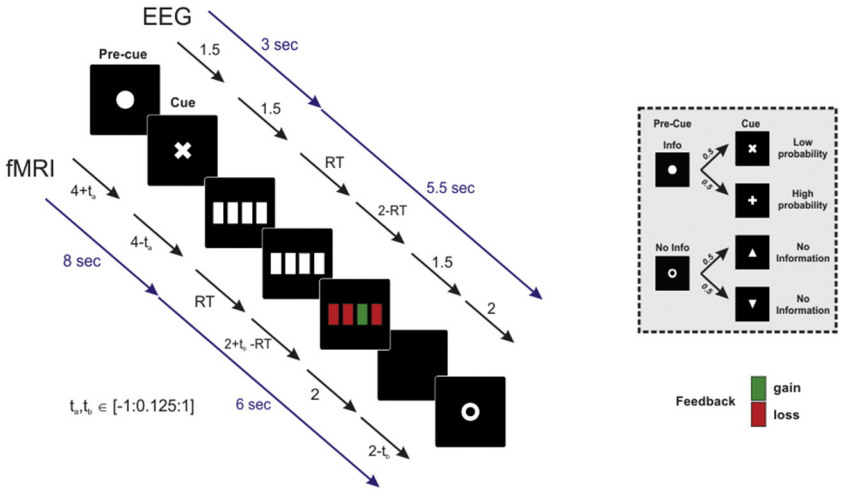

Fig. 1. Gambling task. Experimental setup for the gambling task with the different timings and jitter for the two modalities (EEG, fMRI).

Unknown to the subjects, the characteristics of the trial and its result (gain or loss) were decided by the computer program before the start of the experiment. In the fMRI task, participants completed five runs of 700 s, with 24 informative and 24 non-informative trials each. Twelve of the informative trials corresponded to high probability of winning: eight yielded a gain and four yielded a loss [$p(gain) = 8/12 = 0.67$, slightly smaller than if the cards were chosen at random $p(gain) = ¾ = 0.75$]. The other twelve informative trials were low probability gain trials with eight loss trials and four gain trials [$p(gain) = 4/12 = 0.33$]. In half of the non-informative trials, three green cards and one red card appeared in the screen while in the other half of the trials there were three red cards and one green card. Overall, non-informative trials presented equal probability of gaining and loosing [p(gain) = 0.5]. Therefore, in each of the five runs, 24 gain and 24 loss trials occurred (a total of 120 gains and 120 losses). The colors that represented gains and losses during feedback (green vs. red) were counterbalanced among subjects to eliminate any possible color confound. The EEG task structure was similar to the fMRI task, adapted to the characteristics of the technique (that is, with more trials and reduced event time). Therefore, the task consisted in 600 trials, 300 informative trials and 300 non-informative trials. From the informative trials, 150 were high probability of winning (100 gain trials and 50 loss trials, $p(gain) = 0.67$) and 150 were low probability of winning (50 gain trials and 100 loss trials, $p(loss) = 0.33$). For the non-informative, 150 were gain trials and 150 were loss trials. Therefore, in the EEG task 300 gain and 300 loss trials occurred. Since the same number of gains and losses were presented in both modalities (120 for fMRI and 300 for EEG), a participant that always responded to the stimuli would earn zero Euros at the end of the experiment. The only way participants could win or lose money at the end of the experiment was given by the no answered trials which could alter the balance among gains and losses (e.g., in the fMRI task, a participant who missed two loss trials would end with 120 gains and 118 losses, thus earning at the end of the experiment 1 Euro).

At the beginning of both sessions, participants were informed about the structure of the trials and about the different meaning of the pre-cues and cues. In addition, they performed some practice trials to correctly understand the task. In conclusion, for both fMRI and EEG, the task had the same structure, which only differed in the number of gain and loss trials and in the timings of the stimuli and jitters. These modifications were applied to adapt to the different technical requirements of each neuroimaging modality (see Carlson et al., 2011 for a similar procedure involving EEG and fMRI in a gambling task).

EEG Data Acquisition

EEG was recorded in a separate session, using a BrainAmp amplifier. Tin electrodes mounted in an electrocap (Electro-Cap International), located at 29 standard positions (Fp1/2, Fz, F7/8, F3/4, Fc1/2 Fc5/6, Cz, C3/4, T3/4, Cp1/2, Cp5/6, Pz, P3/4, T5/6, PO1/2, O1/2) and left and right mastoids. An electrode placed at the lateral outer canthus of the right eye served as an online reference. EEG was re-referenced offline to the linked mastoids. Vertical eye movements were monitored with an electrode at the infraorbital ridge of the right eye. Electrode impedances were kept below 5 kΩ. The electrophysiological signals were filtered with a highpass filter at 0.01 Hz (half-amplitude cutoffs) and digitized at a rate of 500 Hz. Data was low-pass filtered offline at 80 Hz. Trials with absolute mean amplitude higher than 100 μV were automatically rejected off-line (M = 88.5% of the trials were included in the analysis; Gains = 88.8% ± 13.85; Losses = 88.2% ± 13.89; $t(19) = 1.5$, $p = .14$).

fMRI Data Acquisition

fMRI data were collected on a separate session from EEG using a 3-T whole-body MRI scanner (Siemens Magnetom Trio, Erlangen, Germany). High-resolution structural images (192 sagittal slices, TR = 2500 ms, TE = 4.77 ms, IT = 1100 ms, flip-angle = 7, 1-mm isotropic voxels) were followed by five runs of 350 sequential whole-brain functional images sensitive to the blood oxygenation level-dependent contrast (echo planar T2-weighted gradient echo sequence, TR = 2000 ms, TE = 30 ms, matrix = 128 × 128, 32 axial slices, 2 mm in-plane resolution, 4 mm thickness, no gap).

EEG Analysis

TF data associated with feedback-evaluation was extracted for positive and negative outcomes. TF analysis was performed in single trial 4-s epochs (−2 s prior feedback to 2 s after it) using 7-cycle complex Morlet wavelets. Changes in time varying energy (square of the convolution between wavelet and signal) in the studied frequencies (from 1 to 40 Hz; linear increase) were computed for each trial. Trials of the same condition (gains and losses) were averaged for each subject and baseline corrected before performing a grand average with all the individuals. The baseline was defined 100 ms prior to feedback onset (−100 to 0 ms.). The averaged oscillatory activity from this period was used to correct power increases on each frequency following feedback onset. The baseline values were subtracted from all time–frequency values of the epoch and the outcome was divided by the baseline values. With this procedure we obtained changes in power with respect to the baseline, highlighting stimulus-induced changes in oscillatory power. The electrodes were selected based on visual inspection of the topographical maps of BOA for the group average difference between gains and losses. The time course of BOA in the gain–loss TF contrast was extracted from the same electrodes for all participants.

fMRI Analysis

Data were analyzed using standard procedures implemented in the Statistical Parameter Mapping software (SPM8, Wellcome Department of Imaging Neuroscience, University College, London, UK, www.fil.ion.ucl.ac.uk/spm/). The preprocessing included slice timing, realignment, segmentation (Ashburner and Friston, 2005), normalization and smoothing with an 8 mm Gaussian kernel.

A general linear model least-square estimation by modeling the different conditions with a regressor waveform convolved with a canonical hemodynamic response function was used. An event-related design matrix was created including the following conditions of interest: informative pre-cue, non-informative pre-cue, high probability cue, low probability cue, non-informative cue, cards (modeled at the moment in which the 4 cards were shown), response choice (modeled at the moment in which the subjects selected one card), low probability loss, high probability loss, non-informative loss, low probability gain, high probability gain, and non-informative gain (the last six modeled at the moment in which feedback was provided). Confounding factors from head movement were also included in the model. After model estimation, the general Gain > Loss and Loss > Gain contrasts (including gain and loss trials from high, low and random probability conditions) were calculated for each subject.

First level contrasts were entered into a second level one sample t-test in order to calculate group effects. All activations are reported in the tables and figures, unless otherwise noted, at an uncorrected $p < 0.001$ threshold with 100 voxels of cluster extent (Lieberman and Cunningham, 2009).

TF-fMRI Data Fusion

The Fusion ICA Toolbox (http://icatb.sourceforge.net/; which implements Joint ICA; Calhoun et al., 2006) was used to fuse TF components (derived from EEG time courses) with the contrasts of the fMRI images. This method has provided meaningful results in several studies combining multiple data types (Calhoun et al., 2006; Eichele et al., 2008;

Moosmann et al., 2008; Doñamayor et al., 2012) and has been recently validated for separated EEG and fMRI sessions (Mijovic et al., 2012). Joint ICA assumes joint temporal and spatial independence constraints of the TF and fMRI modalities, respectively, to fuse oscillatory and hemodynamic data. It simultaneously identifies the components from both modalities at the same time (Calhoun et al., 2006). Although originally it was applied to fuse EEG with fMRI data (Calhoun et al., 2006, 2009) it has also been used to fuse information between very different modalities, such as MEG and diffusion tensor imaging (Stephen et al., 2013). In our analysis, Joint ICA used individual BOA time-courses (the BOA time-course between 27 and 33 Hz for the Gain > Loss contrast of each subject) in the temporal domain and individual activation maps (the fMRI Gain > Loss image contrast of each participant) in the spatial domain. Joint ICA assumes that the components extracted from both modalities will co-vary, either because they are generated by the same brain area, or due to the fact that the regions showing enhanced fMRI signal for the contrast of interest (Gain > Loss) have a participatory role in the oscillatory activity without being the main source of it (Mijovic et al., 2012). Using the Infomax algorithm (Bell and Sejnowski, 1995), the independence between spatial fMRI and temporal TF components was maximized and both their shared unmixing matrix and the fused TF and fMRI sources were calculated. A Joint ICA analysis was calculated combining individual time courses of beta power changes with subject specific Gain > Loss fMRI contrasts (the Loss > Gain fMRI contrast did not reach significance, see Results). A complementary analysis, combining theta power changes with subject specific Gain > Loss fMRI contrasts was also calculated, in order to assess the specificity of beta coupling on gains. The number of independent joint TF-fMRI components was set to 12 (Calhoun et al., 2006). Once calculated, TF components were first regressed against the mean power time course and then ranked according to their contribution to the latter. The component with the maximum contribution was further analyzed. The corresponding fMRI components were scaled to Z scores and thresholded at $p < 0.001$ ($Z > 3.1$) and 100 voxels of spatial extent (Doñamayor et al., 2012).

Results

Time–Frequency

Fig. 2A shows the time–frequency power changes following gains, losses and the difference between both conditions. As observed, there was a clear enhancement of BOA following positive compared to negative feedback, with its maximum between 27–33 Hz and between 280 and 320 ms. Topographical representation revealed a mid-frontal scalp distribution of the BOA, slightly lateralized to the right (as in Cunillera et al., 2012 and HajiHosseini et al., 2012), with a maximum at Cz and Fc2 locations (Fig. 2B). Additionally, and in agreement with previous studies (Mas-Herrero and Marco-Pallarés, 2014), mid-frontal theta activity (4–8 Hz) was enhanced following negative compared to positive feedback between 200 and 550 ms.

A Repeated-Measures ANOVA with electrodes (Cz and Fc2) and valence (gain and losses) as within-participant factors was performed with BOA changes (27–33 Hz) averaged from 280 to 320 ms. The analysis revealed a significant enhancement of BOA following positive feedback [valence effect: $F(1, 19) = 5.02$, $p = .037$]. Therefore, and replicating previous findings, gains evoked greater BOA power increases than losses. This effect was similar at both Fc2 and Cz electrodes [electrode effect: $F(1, 19) = .07$, $p = .79$; electrode × valence: $F(1, 19) = 1.2$, $p = .3$].

fMRI

The Gain > Loss contrast yielded the expected activations in reward-related areas, especially in bilateral ventral striatum and ventromedial PFC and also in bilateral hippocampi (activation in these reward related areas survived a $p < 0.001$ FWE-corrected threshold at the cluster level; see Fig. 2B and Table 1). At the selected threshold, the Loss > Gain contrast yielded no significant activations, suggesting that a similar brain network is involved in processing both gains and losses but with a differential amount of activation (increasing with gains and decreasing with losses; Dreher, 2007; Tom et al., 2007; Ripollés et al., 2014; Càmara et al., 2009 and Càmara et al., 2010). Thus, this contrast was not further analyzed.

fMRI-TF Fusion

The maximum TF component extracted for the BOA-Gain > Loss joint analysis (see Fig. 3 right panel, the maximum TF component is depicted in orange; mean BOA time-course from Fig. 2 is depicted in blue), yielded a corresponding fMRI spatial map with significant brain activations at the bilateral ventral striatum and hippocampi, the left ventrolateral prefrontal cortex (BA 47, inferior frontal gyrus) and left precentral gyrus (BA 6), extending to portions of the dorsolateral prefrontal

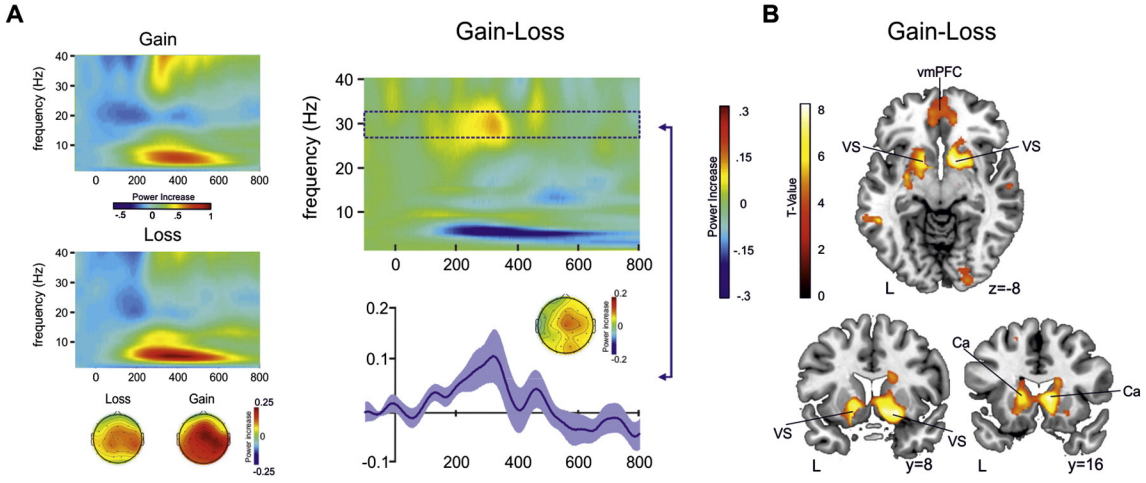

Fig. 2. A. Main TF results. Time–frequency plots for gain, loss and the difference between both conditions averaged over FC2 and Cz. Note that beta oscillatory activity is increased in gains compared to losses. In particular, the greatest difference between both conditions was present between 27 and 33 Hz. The time course of BOA difference (averaged between 27 and 33 Hz) and the topographical maps are also represented. Power increases indicate relative changes respect the baseline. B. Main fMRI results. In red–yellow, enhanced group-level fMRI-signal for the Gain > Loss contrast ($p < 0.001$ uncorrected, 100 voxels of spatial extent; ventral striatum activation is $p < 0.001$ FWE-corrected at the cluster level). Neurological convention is used with MNI (Montreal Neurological Institute) coordinates at the bottom right of each slice. VS, ventral striatum; vmPFC, ventromedial prefrontal cortex; Ca, caudate; L, left hemisphere; R, right hemisphere.

Table 1
Effects of monetary gains on fMRI signal: enhanced group level fMRI-signals for the Gain > Loss contrast thresholded at an uncorrected $p < 0.001$ with 100 voxels of cluster extent (see also Fig. 2B). MNI coordinates are used. For better location of the different regions, several peak voxels are reported for each cluster. BA, Brodmann area.

Anatomical area	Size	Coordinates	t-value
Right putamen;	5203*	22 10 −10	8.33
Right ventral striatum;		12 6 −10	8.08
Right caudate;		10 16 4	7.83
Left ventral striatum;		−16 6 −14	7.37
Bilateral anterior cingulate cortex (BA 24, 32);		−4 42 0	7.07
Left middle frontal gyrus (BA 10);		−30 62 8	7.05
Left caudate;		−14 16 4	6.80
Ventro-medial prefrontal cortex (BA 10, 11, 32);		−6 50 −4	6.08
Left hippocampus;		−32 −22 −18	6.04
Left putamen;		−28 −6 −6	5.77
Right hippocampus.		18 −10 −14	4.73
Left middle/superior frontal gyrus (BA 10).	523*	−18 26 64	6.82
Right superior temporal gyrus (BA 22).	122	58 −16 −2	6.28
Right cerebellum.	231*	8 −80 −44	5.94
Left middle temporal gyrus (BA 21).	155	−52 −42 −6	5.89
Bilateral middle/posterior cingulate gyrus (BA 23, 31).	365*	−6 −46 36	5.70
Right inferior/middle occipital gyrus (BA 18,18);	891*	32 −82 8	5.65
Right calcarine (BA 17).		18 −92 4	5.54
Right inferior parietal gyrus (BA 40).	174*	54 −32 52	5.59
Left inferior parietal gyrus (BA 40).	128	−52 −42 40	5.31
Right cerebellum.	152	34 −68 −32	4.72

* Survived a $p < .05$ FWE correction at the cluster level.

Table 2
Spatial component for the TF-fMRI analysis. fMRI spatial map corresponding to the maximum beta rhythm component extracted, scaled to Z scores and thresholded at $p < 0.001$ ($Z > 3.1$) and 100 voxels of spatial extent (see also Fig. 3). MNI coordinates are used. For better location of the different regions, several peak voxels are reported for each cluster. BA, Brodmann area.

Beta with Gain > Loss fMRI contrast			
Anatomical area	Size	Coordinates	z-Score
L Ventral striatum	409	−18 2 −12	6.54
L Hippocampus		−14 −2 −16	4.99
L Amygdala		−20 −2 −14	4.82
L Putamen		−16 12 −4	4.62
L Caudate		−10 16 −2	3.30
L Parietal gyrus (BA 7)	170	−28 −72 50	6.10
L Precental/middle frontal gyrus (BA 6,9)	207	−50 −4 42	5.01
R Ventral striatum	221	18 4 −14	4.68
R Hippocampus		14 −6 −16	3.75
R Putamen		22 10 −4	3.49
R Amygdala		20 0 16	3.21
R Caudate		14 16 8	3.24
L Inferior frontal gyrus (BA 47)	199	−52 16 2	4.50

gyrus (BA 9, middle frontal gyrus) and the left parietal gyrus (see Table 2 and left panel of Fig. 3, red–yellow areas). As expected, the maximum TF component extracted for the theta-Gain > Loss joint analysis yielded no significant activations in its corresponding spatial fMRI map at the selected threshold, supporting the specificity of beta coupling on gains.

Discussion

The goal of the present study was to determine whether BOA is associated to the activation of several reward-related regions during reward processing. We combined the temporal and spectral dynamics of time–frequency analysis of EEG and the high spatial resolution of fMRI by means of a Joint ICA analysis (Calhoun et al., 2006). We found that increases in mid-frontal BOA were coupled with the ventral striatum, hippocampus bilaterally and the left prefrontal cortex. Interestingly, the theta-Gain > Loss Joint ICA analysis yielded no significant correlations with spatial fMRI maps, supporting the specificity of our findings. Present results support the idea that cortical BOA following rewards reflects the cross-talk between attentional, motivational and memory systems (Marco-Pallarés et al., 2014).

Previous studies have showed that beta rhythm is specifically engaged by positive feedback (Cohen et al., 2007; HajiHosseini et al., 2012; Cunillera et al., 2012; Alicart et al., in press) or reward-predicting cues (Bunzeck et al., 2011). The similarities between BOA and dopaminergic neurons responses following rewards has led to the assumption that mesolimbic activations modulate this gain-related signal, a claim that has been indirectly supported by previous studies (Marco-Pallarés et al., 2009; Leicht et al., 2013). In parallel, intra-recording studies have shown that VTA neurons projecting to prefrontal cortex preferentially fire between 20 and 30 Hz, suggesting that dopaminergic projections might indeed generate BOA in prefrontal cortex (Lammel et al., 2008). However, until now, no studies have taken advantage of combined EEG-fMRI analysis to determine whether a direct relationship exists between BOA and the engagement of subcortical reward structures. Our findings further support this proposal. The BOA-associated hippocampal and striatal regions found in the present study are also modulated by dopamine transmission following

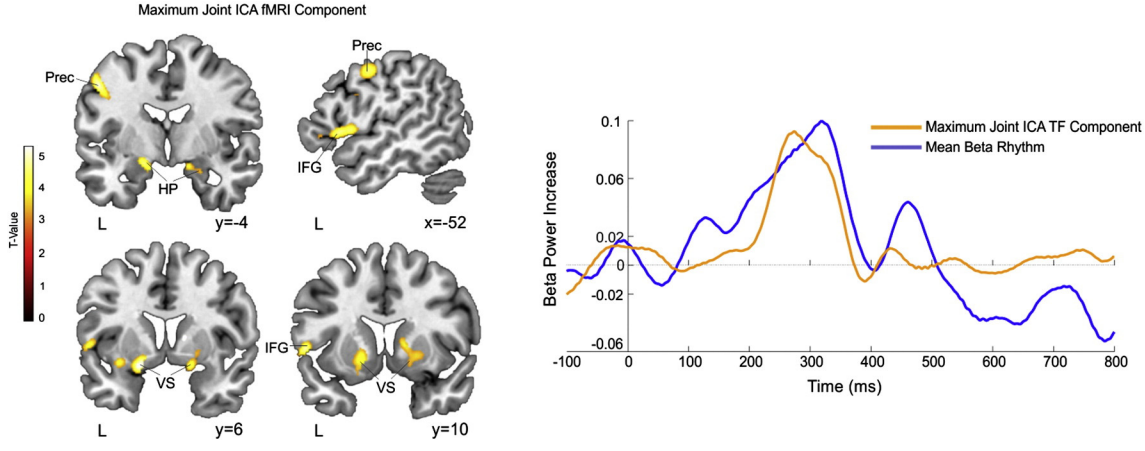

Fig. 3. Main results for the joint TF-fMRI analysis. Neurological convention is used with MNI coordinates at the bottom right of each slice. On the left, the spatial map corresponding to the maximum TF component extracted for the beta rhythm is reported at a $Z > 3.1$ ($p < 0.001$, 100 voxels of cluster extent). On the right, the maximum beta TF component of the Joint ICA analysis (orange) is shown along with the mean beta power increase (from Fig. 2, in blue). VS, ventral striatum; HP, hippocampus; IFG, inferior frontal gyrus; PG, parietal gyrus; Prec, precentral gyrus; L, left hemisphere; R, right hemisphere.

rewarding events (Jay, 2003; Schott et al., 2008). In particular, this dopaminergic transmission may enhance memory processes in rewarding contexts by modulating the entrance of information into the hippocampus (Wittmann et al., 2005; Adcock et al., 2006) through fronto–striatal supervision (Murty and Adcock, 2013; McNab and Kingberg, 2008). On that sense, fronto–striatal interactions between dorsolateral and, specially, ventrolateral prefrontal cortices with the striatum (as those identified in the present study) are thought to be involved in the selection and prioritization of behaviorally relevant information for storage in memory (Murty and Adcock, 2013; McNab and Kingberg, 2008) while striatal–hippocampal interaction would be crucial to enhance the encoding of such information (Wittmann et al., 2005). Thus, the engagement of fronto–striatal–hippocampal circuits is critical to memory enhancement in reward contexts. Accordingly, electrophysiological studies in humans have revealed that memory improvements in reward contexts are also accompanied by increases of mid-frontal BOA power (Kawasaki and Yamaguchi, 2013), supporting the functional relationship between BOA and fronto–striatal–hippocampal circuits involved in memory enhancing and learning (Marco-Pallarés et al., 2014).

Furthermore, similar fronto–striatal–hippocampal networks have been suggested to be engaged during novelty processing (Wittmann et al., 2007). Remarkably, contextual novelty modulates cortical BOA in response to reward-predicting cues (Bunzeck et al., 2011), supporting the idea that both reward and novelty processing may engage similar networks, which might be coordinated through BOA. In parallel, bursts of beta oscillations have also been reported during exploration of novel environments in the hippocampus (Berke et al., 2008) and after reward delivery in the striatum (Howe et al., 2011).

In agreement with Marco-Pallarés and colleagues' proposal (2014), we suggest that BOA might reflect the engagement of prefrontal cortex under dopaminergic modulation. This engagement might enhance fronto–striatal coupling, which in turn may facilitate the entrance of behavioral relevant information into memory by promoting striatal–hippocampal interactions. Thus, BOA would be a key mechanism for integrating information of all these distributed networks involved in reward-guided learning. However, it is worth mentioning that so far, most of the studies have focused on local power changes, which do not necessarily imply long-range communication. Although changes in local power may indeed be related to long-range communication (as observed with theta oscillations, Cohen et al., 2009), further studies analyzing other oscillatory characteristic of BOA, such as phase synchronization, are crucial to understand the relationship between the results obtained with measures of power and long-range synchronization between distant regions.

One potential limitation of our study is that we acquired EEG and fMRI data during separated sessions. However, the effects of monetary gains in gambling tasks—which we replicate here—are very robust and have been widely studied both in EEG and fMRI (Camara et al., 2009, 2010; Ripollés et al., 2014; Carlson et al., 2011; Marco-Pallarés et al., 2008, 2009; Sescousse et al., 2013; Cohen et al., 2007; Padrao et al., 2013). In addition, in the gambling task used in this study, the amounts of overall monetary gains and losses were fixed and equal for all participants and sessions. On the other hand, it is important to note that the use of different number of trials between neuroimaging modalities, when enough trials are used, does not affect the data fusion, as Joint ICA works with individual averaged data (mean beta response and Gain > Loss contrast of each subject). The fact that we used standard number of trials for both fMRI (our task had 120 gains and losses; Ripollés et al., 2014 used 90 trials and Carlson et al., 2011 used 30 gains and losses) and EEG (our task had 600 gains and losses; Padrao et al., 2013 and Vega et al., 2013 used 340 gain and loss trials) and that we replicated previous studies further supports our claim. Finally, a recent study validated the use of Joint ICA when fusing data from separated EEG and fMRI sessions (Mijovic et al., 2012).

In summary, the present study indicates that mid-frontal beta oscillations are associated to different brain areas related to attention, reward and memory, suggesting that BOA might have a role in the coordination of reward networks.

Acknowledgments

The present project has been funded by the Spanish Government (MINECO Grants PSI2012-37472 to J.M.P., PSI2011-29219 to A.R.F., FPI program BES-2010-032702 to E.M.-H. and FPU program AP2010-4179 to P.R.). The funders had no role in study design, data collection and analysis, decision to publish, or preparation of the manuscript.

References

Adcock, R.A., Thangavel, A., Whitfield-Gabrieli, S., Knutson, B., Gabrieli, J.D., 2006. Reward-motivated learning: mesolimbic activation precedes memory formation. Neuron 50, 507–517.
Alicart, H., Cucurell, D., Mas-Herrero, E., Marco-Pallarés, J., 2015. Human oscillatory activity in near-miss events. Soc. Cogn. Affect. Neurosci. (nsv033, in press).
Apitz, T., Bunzeck, N., 2014. Early effects of reward anticipation are modulated by dopaminergic stimulation. PloS One 9, e108886.
Ashburner, J., Friston, K.J., 2005. Unified segmentation. Neuroimage 26, 839–851.
Bell, A.J., Sejnowski, T.J., 1995. An information-maximization approach to blind separation and blind deconvolution. Neural Comput. 7, 1129–1159.
Berke, J.D., Hetrick, V., Breck, J., Greene, R.W., 2008. Transient 23-30 Hz oscillations in mouse hippocampus during exploration of novel environments. Hippocampus 18, 519–529.
Blanchard, M.M., Mendelsohn, D., Stamp, J.A., 2009. The HR/LR model: further evidence as an animal model of sensation seeking. Neurosci. Biobehav. Rev. 33, 1145–1154.
Bunzeck, N., Guitart-Masip, M., Dolan, R.J., Duzel, E., 2011. Contextual novelty modulates the neural dynamics of reward anticipation. J. Neurosci. 31, 12816–12822.
Calhoun, V.D., Adali, T., Pearlson, G.D., Kiehl, K.A., 2006. Neuronal chronometry of target detection: fusion of hemodynamic and event-related potential data. Neuroimage 30, 544–553.
Calhoun, V.D., Liu, J., Adali, T., 2009. A review of group ICA for fMRI data and ICA for joint inference of imaging, genetic, and ERP data. Neuroimage 45, S163–S172.
Camara, E., Rodriguez-Fornells, A., Ye, Z., Munte, T.F., 2009. Reward networks in the brain as captured by connectivity measures. Front. Neurosci. 3, 350–362.
Camara, E., Kramer, U.M., Cunillera, T., Marco-Pallarés, J., Cucurell, D., Nager, W., Mestres-Misse, A., Bauer, P., Schule, R., Schols, L., Tempelmann, C., Rodriguez-Fornells, A., Munte, T.F., 2010. The effects of COMT (Val108/158Met) and DRD4 (SNP -521) dopamine genotypes on brain activations related to valence and magnitude of rewards. Cereb. Cortex 20, 1985–1996.
Carlson, J.M., Foti, D., Mujica-Parodi, L.R., Harmon-Jones, E., Hajcak, G., 2011. Ventral striatal and medial prefrontal BOLD activation is correlated with reward-related electrocortical activity: a combined ERP and fMRI study. Neuroimage 57, 1608–1616.
Cohen, M.X., Elger, C.E., Ranganath, C., 2007. Reward expectation modulates feedback-related negativity and EEG spectra. Neuroimage 35, 968–978.
Cohen, M.X., Axmacher, N., Lenartz, D., Elger, C.E., Sturm, V., Schlaepfer, T.E., 2009. Nuclei accumbens phase synchrony predicts decision-making reversals following negative feedback. J. Neurosci. 29 (23), 7591–7598.
Cohen, M.X., Wilmes, K., Vijver, I., 2011. Cortical electrophysiological network dynamics of feedback learning. Trends Cogn. Sci. 15, 558–566.
Cunillera, T., Fuentemilla, L., Perianez, J., Marco-Pallarés, J., Kramer, U.M., Camara, E., Munte, T.F., Rodriguez-Fornells, A., 2012. Brain oscillatory activity associated with task switching and feedback processing. Cogn. Affect. Behav. Neurosci. 12, 16–33.
Dayan, P., Balleine, B.W., 2002. Reward, motivation, and reinforcement learning. Neuron 36, 285–298.
Doñamayor, N., Heilbronner, U., Munte, T.F., 2012. Coupling electrophysiological and hemodynamic responses to errors. Hum. Brain Mapp. 33, 1621–1633.
Dreher, J.C., 2007. Sensitivity of the brain to loss aversion during risky gambles. Trends Cogn. Sci. 11, 270–272.
Eichele, T., Calhoun, V.D., Moosmann, M., Specht, K., Jongsma, M.L., Quiroga, R.Q., Nordby, H., Hugdahl, K., 2008. Unmixing concurrent EEG-fMRI with parallel independent component analysis. Int. J. Psychophysiol. 67, 222–234.
HajiHosseini, A., Rodriguez-Fornells, A., Marco-Pallarés, J., 2012. The role of beta-gamma oscillations in unexpected rewards processing. Neuroimage 60, 1678–1685.
Howe, M.W., Atallah, H.E., McCool, A., Gibson, D.J., Graybiel, A.M., 2011. Habit learning is associated with major shifts in frequencies of oscillatory activity and synchronized spike firing in striatum. Proc. Natl. Acad. Sci. U. S. A. 108, 16801–16806.
Jay, T.M., 2003. Dopamine: a potential substrate for synaptic plasticity and memory mechanisms. Prog. Neurobiol. 69, 375–390.
Kawasaki, M., Yamaguchi, Y., 2013. Frontal theta and beta synchronizations for monetary reward increase visual working memory capacity. Soc. Cogn. Affect. Neurosci. 8 (5), 523–530.
Lammel, S., Hetzel, A., Häckel, O., Jones, I., Liss, B., Roeper, J., 2008. Unique properties of mesoprefrontal neurons within a dual mesocorticolimbic dopamine system. Neuron 57, 760–773.
Leicht, G., Troschütz, S., Andreou, C., Karamatskos, E., Ertl, M., Naber, D., Mulert, C., 2013. Relationship between oscillatory neuronal activity during reward processing and trait impulsivity and sensation seeking. PLoS One 8, e83414.
Lieberman, M.D., Cunningham, W.A., 2009. Type I and Type II error concerns in fMRI research: re-balancing the scale. Soc. Cogn. Affect. Neurosci. 4, 423–428.

Luft, C.D., Nolte, G., Bhattacharya, J., 2013. High-learners present larger mid-frontal theta power and connectivity in response to incorrect performance. J. Neurosci. 33, 2029–2038.
Marco-Pallarés, J., Cucurell, D., Cunillera, T., Garcia, R., Andres-Pueyo, A., Munte, T.F., Rodriguez-Fornells, A., 2008. Human oscillatory activity associated to reward processing in a gambling task. Neuropsychologia 46, 241–248.
Marco-Pallarés, J., Cucurell, D., Cunillera, T., Kramer, U.M., Camara, E., Nager, W., Bauer, P., Schule, R., Schols, L., Munte, T.F., Rodriguez-Fornells, A., 2009. Genetic variability in the dopamine system (dopamine receptor D4, catechol-O-methyltransferase) modulates neurophysiological responses to gains and losses. Biol. Psychiatry 66, 154–161.
Marco-Pallarés, J., Munte, T.F., Rodriguez-Fornells, A., 2014. The role of high-frequency oscillatory activity in reward processing and learning. Neurosci. Behav. Rev. 49, 1–7.
Mas-Herrero, E., Marco-Pallarés, J., 2014. Frontal theta oscillatory activity is a common mechanism for the computation of unexpected outcomes and learning rate. J. Cogn. Neurosci. 26, 447–458.
McNab, F., Kingberg, T., 2008. Prefrontal cortex and basal ganglia control access to working memory. Nat. Neurosci. 11, 103–107.
Mijovic, B., Vanderperren, K., Novitskiy, N., Vanrumste, B., Stiers, P., Bergh, B.V., Lagae, L., Sunaert, S., Wagemans, J., Huffel, S.V., Vos, M.D., 2012. The "why" and "how" of JointICA: results from a visual detection task. Neuroimage 60, 1171–1185.
Moosmann, M., Eichele, T., Nordby, H., Hugdahl, K., Calhoun, V.D., 2008. Joint independent component analysis for simultaneous EEG-fMRI: principle and simulation. Int. J. Psychophysiol. 67, 212–221.
Murty, V.P., Adcock, R.A., 2013. Enriched encoding: reward motivation organizes cortical networks for hippocampal detection of unexpected events. Cereb. Cortex 24, 160–168.
Padrao, G., Mallorqui, A., Cucurell, D., Marco-Pallarés, J., Rodriguez-Fornells, A., 2013. Neurophysiological differences in reward processing in anhedonics. Cogn. Affect. Behav. Neurosci. 13, 102–115.
Ripollés, P., Marco-Pallarés, J., Hielscher, U., Mestres-Missé, A., Tempelmann, C., Heinze, H.J., Rodriguez-Fornells, A., Noesselt, T., 2014. The role of reward in word learning and its implications for language acquisition. Curr. Biol. 24, 2606–2611.
Schott, B.H., Minuzzi, L., Krebs, R.M., Elmenhorst, D., Lang, M., Winz, O.H., Seidenbecher, C.I., Coenen, H.H., Heinze, H.J., Zilles, K., Duzel, E., Bauer, A., 2008. Mesolimbic functional magnetic resonance imaging activations during reward anticipation correlate with reward-related ventral striatal dopamine release. J. Neurosci. 28, 14311–14319.
Sescousse, G., Caldu, X., Segura, B., Dreher, J.C., 2013. Processing of primary and secondary rewards: a quantitative meta-analysis and review of human functional neuroimaging studies. Neurosci. Biobehav. Rev. 37, 681–696.
Stephen, J.M., Coffman, B.A., Jung, R.E., Bustillo, J.R., Aine, C.J., Calhoun, V.D., 2013. Using Joint ICA to link function and structure using MEG and DTI in schizofrenia. Neuroimage 83, 418–430.
Tom, S.M., Fox, C.R., Trepel, C., Poldrack, R.A., 2007. The neural basis of loss aversion in decision-making under risk. Science 315, 515–518.
Vega, D., Soto, A., Amengual, J.L., Ribas, J., Torrubia, R., Rodriguez-Fornells, A., Marco-Pallarés, J., 2013. Negative reward expectations in Borderline Personality Disorder patients: neurophysiological evidence. Biol. Psychol. 94, 388–396.
von Stein, A., Sarnthein, J., 2000. Different frequencies for different scales of cortical integration: from local gamma to long range alpha/theta synchronization. Int. J. Psychophysiol. 38 (3), 301–313.
Wittmann, B.C., Schott, B.H., Guderian, S., Frey, J.U., Heinze, H.J., Duzel, E., 2005. Reward-related FMRI activation of dopaminergic midbrain is associated with enhanced hippocampus-dependent long-term memory formation. Neuron 45, 459–467.
Wittmann, B.C., Bunzeck, N., Dolan, R.J., Duzel, E., 2007. Anticipation of novelty recruits reward system and hippocampus while promoting recollection. Neuroimage 38, 194–202.
Wittmann, B.C., Schiltz, K., Boehler, C.N., Duzel, E., 2008. Mesolimbic interaction of emotional valence and reward improves memory formation. Neuropsychologia 46, 1000–1008.